RESEARCH ARTICLE

Dynamics of Zebrafish Somitogenesis

Christian Schröter,[1] Leah Herrgen,[1] Albert Cardona,[2] Gary J. Brouhard,[1] Benjamin Feldman,[3] and Andrew C. Oates[1]*

Vertebrate somitogenesis is a rhythmically repeated morphogenetic process. The dependence of somitogenesis dynamics on axial position and temperature has not been investigated systematically in any species. Here we use multiple embryo time-lapse imaging to precisely estimate somitogenesis period and somite length under various conditions in the zebrafish embryo. Somites form at a constant period along the trunk, but the period gradually increases in the tail. Somite length varies along the axis in a stereotypical manner, with tail somites decreasing in size. Therefore, our measurements prompt important modifications to the steady-state Clock and Wavefront model: somitogenesis period, somite length, and wavefront velocity all change with axial position. Finally, we show that somitogenesis period changes more than threefold across the standard developmental temperature range, whereas the axial somite length distribution is temperature invariant. This finding indicates that the temperature-induced change in somitogenesis period exactly compensates for altered axial growth. *Developmental Dynamics 237:545–553, 2008.*

Key words: zebrafish; somitogenesis; oscillator; period; frequency; rate; time-lapse; temperature; segmentation; Clock and Wavefront model

Accepted 13 November 2007

INTRODUCTION

Vertebrate somitogenesis is a repeated patterning process that occurs sequentially along the axis of the developing embryo. Current hypotheses of somitogenesis posit a genetic oscillator, termed the segmentation clock, in the presomitic mesoderm (PSM) and tail bud that interacts with a posterior-moving determination wavefront to set the periodic spacing of somite boundaries: this is termed the Clock and Wavefront model (Cooke and Zeeman, 1976; Dubrulle and Pourquie, 2004a; Aulehla and Pourquie, 2006). In this model, somitogenesis period, i.e., the time interval between formation of each successive boundary, is determined by the period of the genetic oscillator, and somite length is the distance traveled by the wavefront in one period of oscillation. Despite increased interest in the underlying molecular processes, the morphological outputs of the clock and the wavefront, somitogenesis period and somite length, have not yet been quantified simultaneously in any species. To understand somitogenesis, as well as other iterative processes during development, a precise quantitative description is necessary.

Estimates of somitogenesis period in several species indicate that there are distinct species-specific dynamics (Pearson and Elsdale, 1979; Tam, 1981; Hanneman and Westerfield, 1989; Brooks and Johnson, 1994; Wood and Thorogood, 1994; Johnston et al., 1995; Schubert et al., 2001). However, the influence of genetic heterogeneity on the period within a single species has not been explored. Furthermore, although most studies report some axial variation of somitogenesis period, conflicting data exist on the axial extent of such changes (Cooke and Zeeman, 1976; Pearson and Elsdale, 1979; Hanneman and Westerfield, 1989; Kimmel et al., 1995; Schmidt and Starck, 2004).

The Supplementary Material referred to in this article can be found at http://www.interscience.wiley.com/jpages/1058-8388/suppmat

[1]Max Planck Institute of Molecular Cell Biology and Genetics, Dresden, Germany
[2]Department of Molecular, Cell, and Developmental Biology, University of California, Los Angeles, California
[3]Medical Genetics Branch, National Institutes of Health, Bethesda, Maryland
Grant sponsor: the Max Planck Society; Grant sponsor: National Institutes of Health.
***Correspondence to: Andrew C. Oates, Max Planck Institute of Molecular Cell Biology and Genetics, Pfotenhauerstr. 108, 01307 Dresden, Germany. E-mail: oates@mpi-cbg.de**

DOI 10.1002/dvdy.21458
Published online 7 February 2008 in Wiley InterScience (www.interscience.wiley.com).

Developmental Dynamics

Kimmel et al. (1995) reported a sudden change in zebrafish trunk somitogenesis period, which has been taken as evidence that different genetic systems pattern anterior and posterior trunk (Holley, 2006), but the period measurements of Hanneman and Westerfield (1989) and Schmidt and Starck (2004) do not support this. Somite length changes along the body axis in the mouse, chick and *Xenopus* embryo (Herrmann et al., 1951; Pearson and Elsdale, 1979; Tam, 1981), but how this correlates with changing period has not been examined. In poikilothermic organisms such as the zebrafish, developmental dynamics, including somitogenesis, depend strongly on temperature (Kimmel et al., 1995). However, the precise temperature dependence of somitogenesis period or somite length has not been investigated systematically.

Time-lapse microscopy has been used to study somitogenesis in various systems, e.g., to observe cell behavior at the forming somite boundary in *Barbus conchonius* (Wood and Thorogood, 1994), zebrafish (Henry et al., 2000), and chick (Kulesa and Fraser, 2002) and to investigate dynamic gene expression patterns during mouse somitogenesis (Masamizu et al., 2006). In each of these cases, only one embryo was imaged at a time, and observations were limited to a single temperature and a small region of the axis. To efficiently gather precise data on global somitogenesis dynamics, an assay system that can document multiple embryos at closely spaced time intervals and defined temperatures throughout the entirety of somitogenesis is required.

Here, we investigate somitogenesis dynamics using the zebrafish model. Because of their transparency and external development, zebrafish embryos allow for easy visualization at high sampling rates without adverse perturbation. In addition, a large number of closely staged embryos can easily be obtained, allowing measurement precision to be estimated. To simultaneously document somitogenesis period and somite length, we used a semiautomatic microscopy setup with a motorized stage that can document approximately 40 zebrafish embryos in parallel throughout somitogenesis. We show that somitogenesis period is constant in the trunk but increases gradually in the tail. Somite length decreases in the posterior body, indicating that wavefront velocity also changes during somitogenesis in the wild-type embryo. Finally, we measure a strong linear dependence of somitogenesis frequency on temperature, whereas somite length distribution is temperature invariant, indicating that the period of the clock compensates for altered growth.

RESULTS

To precisely measure somitogenesis period and somite length, we set out to document multiple embryos developing under the same conditions using brightfield time-lapse microscopy. A motorized stage was used to repeatedly screen up to 41 animals at defined time intervals and at specified, constant temperatures. Applying an ImageJ plugin (for details, see the Experimental Procedures section and Fig. 1A), we automatically generated time-lapse movies of these embryos in parallel (Supplementary Movie S1, which can be viewed at http://www.interscience.wiley.com/jpages/1058-8388/suppmat).

Precise Determination of Somitogenesis Period

The increase in somite number over time can be read from consecutive frames of the movies (Fig. 1B). To determine somitogenesis period, we analyzed the movies, sequentially noting the time at which the boundary posterior to each somite formed. For embryos developing inside the chorion, this approach allowed most trunk somites to be scored. We first analyzed somitogenesis period between somites 6 to 18; the period at other axial positions is described below. Analysis of a single movie gave the somitogenesis period for an individual (Fig. 1C). To examine somitogenesis period as a population property, we analyzed multiple movies that had been recorded in parallel, normalized the data, and calculated the mean formation time, as well as the standard deviation (SD), for each boundary. The uncertainty of the data points, comprising both sampling error and biological variation, remained constant with recording time (Fig. 1D). Linear fits to the data from somites 6 to 18 yielded R^2 values between 0.998 and 0.999, indicating a linear increase in somite number over time. Therefore, a precise estimate of the somitogenesis period (P) for the population could be derived from the slope of the linear curve, which was 24.9 $\pm$ 0.7 min at a temperature of 27.1 $\pm$ 0.1°C for the experiment shown (Fig. 1D). Confidence intervals for fits of comparable experiments were consistently less than 10% of the measured value (Table 1). Therefore, observation of multiple embryos and several boundaries along the axis enabled us to precisely determine the somitogenesis period between somites 6 through 18.

Somitogenesis Period Is Independent of Wild-Type Genetic Background

We next tested the influence of genetic heterogeneity on somitogenesis period. To determine whether the commonly used zebrafish strains (Guryev et al., 2006) have strain-specific period differences, we measured trunk somitogenesis period for the AB strain in direct pairwise comparison to three others: Golden, Wik, and TL (2 experiments per strain, $10 < n < 20$ per strain and experiment). We found no significant difference in somitogenesis period between these strains and the period established for AB (data not shown), suggesting that somitogenesis period is not modified by strain-specific genetic differences.

Somitogenesis Period Is Constant Along the Trunk but Increases in the Tail

While somitogenesis period is constant from somites 6 to 18, the period in the anterior trunk or in the tail might deviate from this behavior. To investigate the extent of axial variation of somitogenesis period, we extended our measurements to the entire embryonic axis.

First, we measured the somitogenesis period of the first 6 somites in comparison to the rest of the trunk, which ends at somite 17. By orienting dechorionated embryos dorsally (Fig. 1A, upper left), we were able to follow somitogenesis in the anterior trunk

(Supplementary Movie S2). In parallel, we documented embryos from the same clutch inside their chorion and followed somitogenesis from a lateral view for the rest of the trunk. We excluded the possibility that dechorionation has adverse effects on the onset or period of somitogenesis by comparing the absolute time when a reference boundary formed in dechorionated vs. undechorionated embryos. When fitting linear curves to the data points obtained from embryos oriented dorsally, we found good linearity (Fig. 2A, red line; $R^2 = 0.9996$). Therefore, somitogenesis period in the anterior trunk can once again be estimated as the slope of the linear fit to the data. The somitogenesis period for somites 1 to 6 (Fig. 2A, red line; $P = 24.7 \pm 5.0$ min) and the period be-

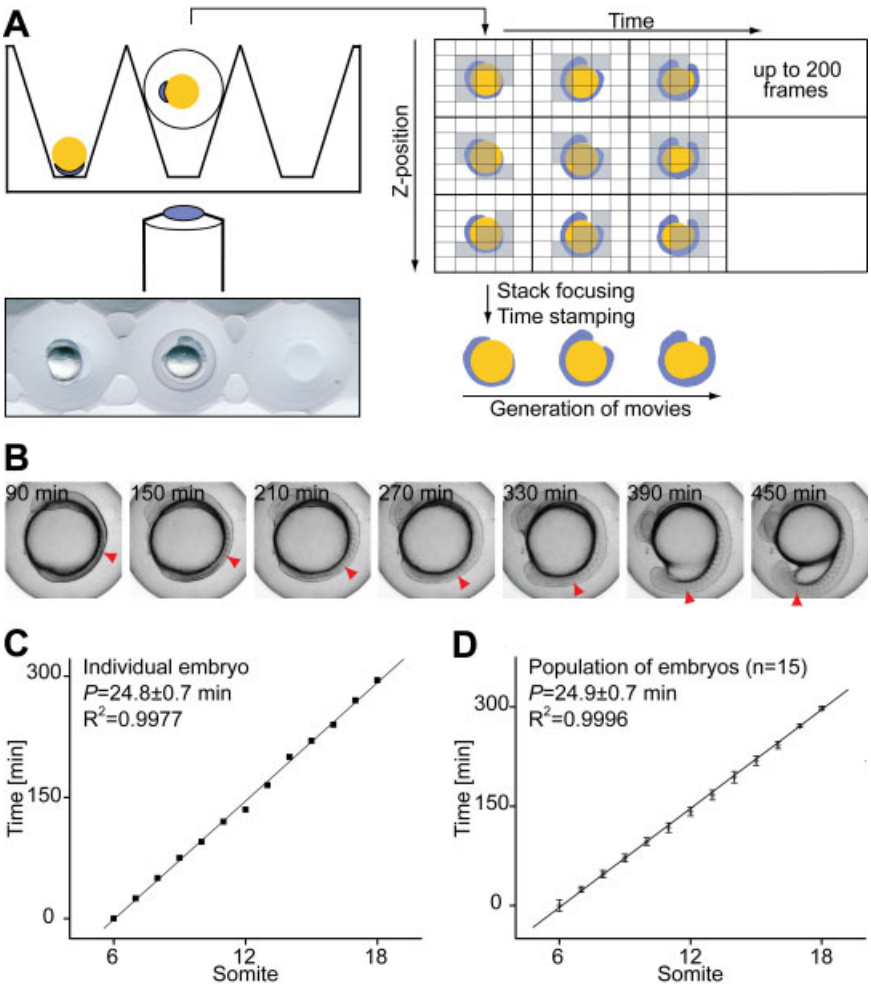

Fig. 1.

Fig. 1. Measurement of trunk somitogenesis period. **A:** Automated generation of somitogenesis time-lapse movies. Embryos in different orientations are held in defined positions in agarose molds. A motorized stage scans through them at defined time intervals. Focused images are generated from Z-stacks using the ImageJ Stack Focuser, and time-stamped QuickTime movies are automatically generated from the focused images. **B:** Single focused frames of a representative movie. Red arrowheads mark the most recently formed somite boundary in each frame. **C:** Period measurement from a single embryo. A movie produced as in A was analyzed from the six-somite stage onward, and formation time of individual somites was normalized relative to somite 6. A linear increase in somite number over time is evident. **D:** Somitogenesis period of the population. The plot shows normalized mean formation times ± SD of boundaries posterior to somite 6 in a group of embryos. Note that the SD does not increase with the duration of recording. The somitogenesis period of the population was estimated as the slope of the linear regression: $P = 24.9 \pm 0.7$ min, $T = 27.1 \pm 0.1$°C.

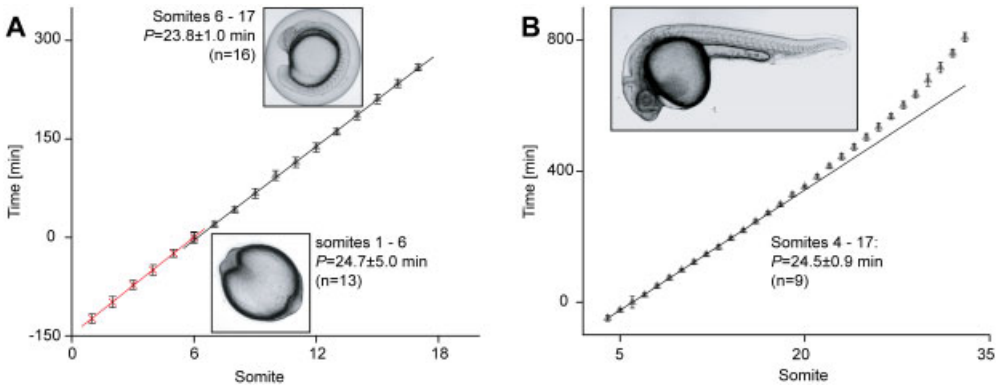

Fig. 2. Somitogenesis period at different axial positions. **A:** Somitogenesis period in the anterior trunk does not differ significantly from the period in the posterior trunk. Populations of embryos from the same clutch were filmed in parallel, either with or without chorion from lateral or dorsal view, respectively. Normalized mean somite formation times ± SD were scored from either set of movies. Linear fits to both data sets (somites 1–6 for the dorsal view, somites 6–17 for the lateral view) yielded slopes that were not significantly different. Note that the limited number of data points for period estimation for the anteriormost somites results in a large confidence interval. $T = 27.6 \pm 0.1$°C. **B:** Somitogenesis period increases in the tail. Tail outgrowth of embryos homozygous for the *nic*^{b107} allele was filmed, and somite formation times were analyzed from somite 4 onward. A linear fit to data points in the trunk region (somites 4–17) indicates nonlinear behavior as somitogenesis proceeds into the tail. $T = 27.4 \pm 0.1$°C.

Developmental Dynamics

tween somites 6 to 17 (Fig. 2A, black line; $P = 23.8 \pm 0.9$ min), were not significantly different, indicating that somites along the entire trunk form with a similar period.

To measure somitogenesis period in the tail, we filmed *nic*^{b107} homozygous embryos, which lack functional nicotinic acetylcholine receptors (Westerfield et al., 1990). Because these embryos are nonmotile and develop otherwise normally far beyond somitogenesis stages (van der Meulen et al., 2005), we could follow tail somitogenesis without anesthetizing the embryo (Supplementary Movie S3). Homozygous *nic*^{b107} embryos did not display significant differences in trunk somitogenesis period compared with their motile littermates, and the difference in somite number by the 28 somite stage between these two groups was less than one (data not shown). Thus, the *nic*^{b107} mutation does not affect somitogenesis period per se. Analysis of the movies showed that, in contrast to the trunk, tail somites formed at continuously longer periods along the axis (Fig. 2B). Thus, somitogenesis period in the tail marks a gradual slowing rather than a separate process with a distinct period. When fitting a linear curve to the data points obtained for trunk somites (4 to 17), we detected the first significant deviations from this fit around somite 20. Therefore, trunk and tail differ in somitogenesis period in the wild-type zebrafish.

Somitogenesis Period Is Linearly Temperature-Dependent

In addition to axial position, environmental temperature is likely to set somitogenesis period in the zebrafish. During the above experiments, we noticed that a minor temperature shift led to a measurable period change (compare Fig. 1C with Fig. 2A). This finding prompted us to explore a larger range of developmental temperatures corresponding to typical laboratory rearing conditions using our time-lapse system. We found that somite number retained a linear relationship with time at all measured temperatures from 20.0°C to 30.8°C (Fig. 3A), whereas the period changed approximately threefold across this range (Table 1). When plotting temperature against somitogenesis frequency, we obtained a good linear relationship (Fig. 3B, $R^2 = 0.9936$). Therefore, the somitogenesis frequency f [somites.h^{-1}] at any temperature T [°C] between 20.0 and 30.8°C can be calculated with the formula $f = aT\text{-}b$, with $a = 0.188 \pm 0.006$ somites.h^{-1}°C^{-1} and $b = 2.7 \pm 0.1$ somites.h^{-1}. Using this formula we can calculate a temperature coefficient Q_{10}, which describes the fold change in the rate of a process across a 10°C interval. The coefficient for somitogenesis in the temperature range from 20°C to 30°C is $Q_{10} = 2.8$.

TABLE 1. Temperature Dependence of Somitogenesis Period[a]

Temperature (°C)	Somitogenesis period (min)	n
20.0 ± 0.4	55.4 ± 1.9	11
20.2 ± 0.4	54.6 ± 2.0	12
22.8 ± 0.5	40.2 ± 1.1	11
24.3 ± 0.1	31.5 ± 0.9	14
27.1 ± 0.1	25.1 ± 0.5	15
27.6 ± 0.1	23.9 ± 0.6	16
29.6 ± 0.2	21.4 ± 1.0	11
30.8 ± 0.3	18.7 ± 1.1	14

[a]Period measurements were performed at different temperatures. Period values are given with 95% confidence intervals and mean temperature ± SD during the recordings. Somitogenesis period was estimated as the slope of the linear regression of the data.

Temperature-Independent Axial Distribution of Somite Length

We next examined the dynamics of somite length at the time of formation (instantaneous length) along the body axis, using movies recorded from a population of *nic*^{b107} homozygous embryos (Fig. 4A). By measuring somites at the time of formation, we exclude contributions of convergent extension or differentiation that mask true somite length if measured later in development. Along the axis, somite length increased slightly in the anterior trunk, remained approximately constant around 50 μm between somites 6 and 14, and decreased thereafter (Fig. 4B). By somite 25, the instantaneous length was approximately 30 μm, almost half that seen in the central trunk. Notably, somite length decreased in the posterior trunk, while somitogenesis period remained constant. Thus, the zebrafish embryo shows a continuous change in the length of the newly forming somites along the axis.

Given our observation of an approximately threefold change of period across the 20.0 to 30.8°C temperature range, we tested whether somite length was affected by temperature. We performed instantaneous somite length measurements in three sets of movies recorded from *nic*^{b107} homozygous embryos at 21.4°C, 25.0°C, and 31.1°C. These measurements did not reveal any consistent change of somite length with temperature (Fig. 4C). Therefore, we conclude that the axial somite length distribution of the zebrafish is independent of steady state temperature.

DISCUSSION

Precision of the Current Technique

Here, we make use of a novel multiple embryo time-lapse imaging protocol to systematically investigate the dynamics of zebrafish somitogenesis at different positions along the developing axis, over a range of temperatures, and in different wild-type strains. By simultaneously recording multiple embryos and scoring multiple boundaries, we obtain precise mean period measurements that allow reliable detection of period differences of ≥10% between groups of embryos, despite the relatively low temporal measurement resolution of each single boundary in a given embryo. Our period measurements in the trunk are in good agreement with some previously

published estimates (Hanneman and Westerfield, 1989; van Eeden et al., 1996; Schmidt and Starck, 2004), although they disagree with a commonly cited study that overestimates the value at 28.5°C (Kimmel et al., 1995). Precision is currently limited by a sampling rate of 5 min, due to the high number of samples and Z-planes and is compounded by uncertainties in the visual analysis of boundary formation. With higher temporal resolution, even subtler period changes could be detected.

We find that genetic polymorphisms between the commonly used zebrafish strains AB, Golden, Wik, and TL (Guryev et al., 2006) do not cause strain-specific differences in mean somitogenesis period. Therefore, we propose that the period is set by a defined complement of genes that may be identified by screening for somitogenesis period mutants using the multiple

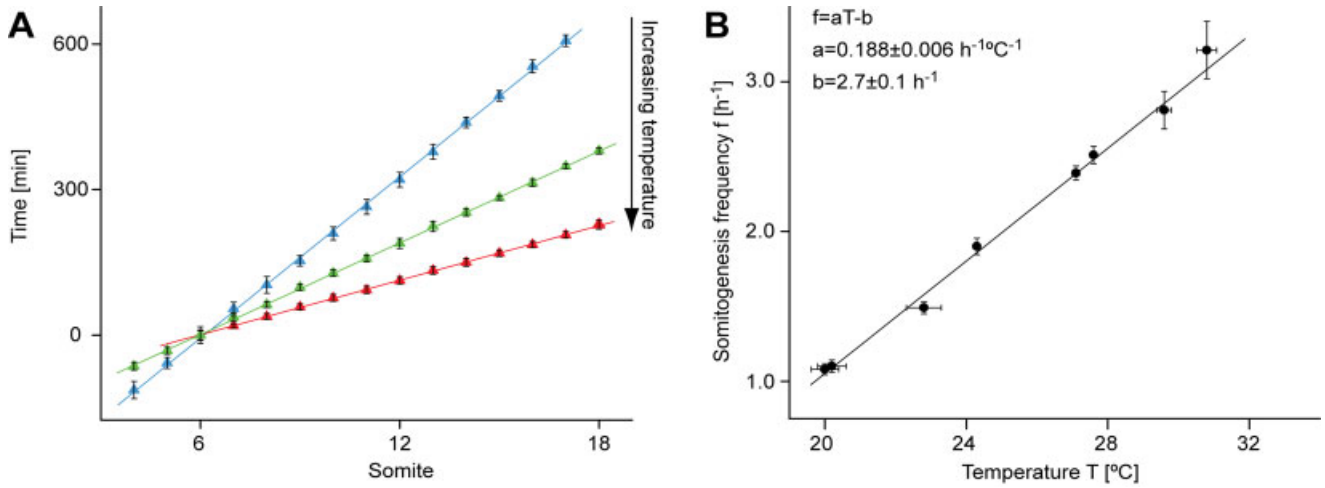

Fig. 3. Temperature dependence of somitogenesis period. **A:** Trunk somite number increases linearly over time at different temperatures. Groups of embryos were filmed at different temperatures. Plotting of mean formation times ± SD for somites 4–18 reveals a linear increase of somite number over time at 20.0°C (blue), 24.3°C (green) and 30.8°C (red). **B:** Somitogenesis frequency depends linearly on temperature. Period values from Table 1 were expressed as frequencies and plotted against the mean temperature during the recording. The fit shows a good linear dependence of frequency and temperature in the range assayed. Error bars show SD of the temperature and 95% confidence interval of the frequency value.

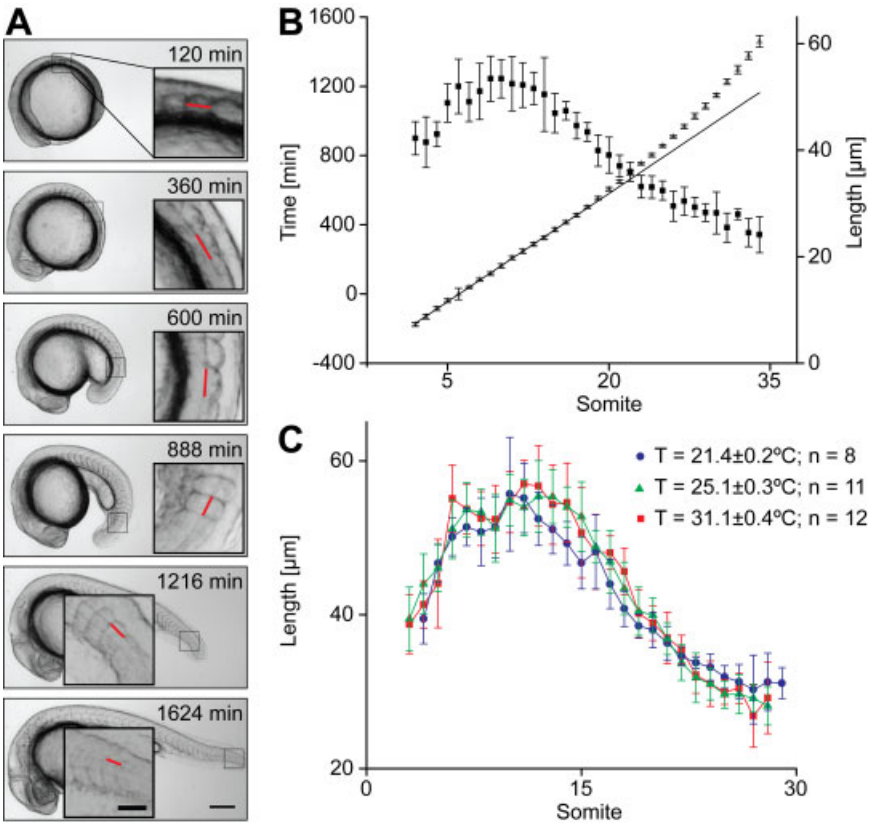

Fig. 4. Axial and temperature dependence of somite length. **A:** Measurement of instantaneous somite length. Somite length was analyzed in focused frames of time-lapse movies by measuring the length of a straight line (red), connecting the intersections of the dorsal limit of the notochord with the two most recently formed somite boundaries. Scale bar = 200 μm in main, 50 μm in inset. **B:** Somite length along the axis is independent of somitogenesis period. Instantaneous somite length (squares) was measured along the entire axis in a population of *nic*^{b107} homozygous embryos and compared with somitogenesis period in the same population (triangles). Somite length increases in the anterior trunk, is approximately constant in the central trunk, and decreases thereafter, independently from somitogenesis period. Error bars show SD of formation time and length measurements. Solid line: Linear fit to estimate somitogenesis period in the trunk. n = 8; P = 41.6 ± 1.2 min; T = 22.7 ± 0.4°C. **C:** Somite length is independent of developmental temperature. Instantaneous somite length was measured in populations of *nic*^{b107} homozygous embryos developing at 21.4°C (blue), 25.0°C (green), and 31.1°C (red). Different temperatures do not lead to a consistent change in instantaneous somite length. Error bars state SD of length measurement.

Developmental Dynamics

embryo time-lapse setup described here. The identification of segmentation period genes would be a major step toward understanding the biochemical basis of rhythmicity in somitogenesis. In addition, measured differences in mean period between wild-type and mutants could be useful for mathematical modeling approaches.

Strong Temperature Dependence of Somitogenesis Period

In the laboratory, zebrafish embryos are commonly raised between 20°C and 30°C (Kimmel et al., 1995; our own unpublished observation), and it is known that temperature has a strong effect on the general speed of development (Kimmel et al., 1995). Here, we precisely quantify the effect of temperature on somitogenesis frequency and find an almost threefold change in the frequency across the standard range of developmental temperatures. Interestingly, in this range, somitogenesis frequency depends linearly on temperature. We provide an equation of the form $f = aT-b$ to estimate somitogenesis frequency (f) for any temperature (T) in this range. At the standard rearing temperature of 28.5°C, we calculate a frequency of 2.7 ± 0.3 somites.h^{-1}, corresponding to a period of 22.6 ± 2.5 min. Additionally, we calculate a temperature coefficient of $Q_{10} = 2.8$ for somitogenesis between 20°C and 30°C. This value agrees well with data obtained for herring (Johnston et al., 1995) and biochemical reactions in vitro, but contrasts to circadian clocks, the free-running periods of which are strongly temperature compensated with a Q_{10} of approximately 1 (Pittendrigh, 1954; Bunning, 1963). The temperature experiments presented in this paper provide a means to directly compare period data collected in different labs, provided temperature can be accurately measured. Finally, our data suggests that, when using period estimates as output variables in mathematical modeling approaches, input variables should be normalized to specific temperatures.

Changes in Somitogenesis Period Along the Developing Axis

For the first time, we have measured somitogenesis period with high precision along the entire axis of a vertebrate species. A rapid start to somitogenesis has been reported in amphioxus and amphibian larvae (Pearson and Elsdale, 1979; Schubert et al., 2001), and there is conflicting evidence concerning the somitogenesis period in the trunk in zebrafish (Hanneman and Westerfield, 1989; Kimmel et al., 1995; Schmidt and Starck, 2004). We find there is a linear increase in somite number over time along the entire zebrafish trunk, indicating no significant differences in somitogenesis period for the first six vs. later trunk somites. In contrast to an earlier proposal of more rapid anterior somitogenesis by Kimmel et al. (1995), the period data presented here eliminates one pillar of the "two genetic systems" hypothesis used to explain posterior specific segmentation defects in Delta-Notch mutant zebrafish lines (Holley, 2006). Instead, our period data are consistent with a single genetic system regulating the timing of trunk somitogenesis, in line with the "rundown" hypothesis first proposed by Jiang et al. (2000), and recently substantiated by Riedel-Kruse et al. (2007).

Somitogenesis in the tail was reported to occur with a longer period than in the trunk in zebrafish (Kimmel et al., 1995; Schmidt and Starck, 2004). Here, we demonstrate and quantify this slowing by measuring somitogenesis period in the *nic*^{b107} strain at high temporal resolution. The increase of period in the tail is gradual, such that it is not possible to exactly define its onset, although it is evident by somite 20. Furthermore, the increase in somite number over time is nonlinear, indicating that there is no sudden transition or switch to a different period. An increase of somitogenesis period in the tail has also been noted in plaice (Brooks and Johnson, 1994), mouse (Tam, 1981) and amphioxus (Schubert et al., 2001), but not in the amphibians *Xenopus* or *Rana* (Pearson and Elsdale, 1979). These data indicate that an increase in tail somitogenesis period is likely the ancestral condition in vertebrates.

Temperature Compensation of Axial Somite Length Distribution

The distribution of instantaneous somite length along the zebrafish axis shows a characteristic signature: Somite length increases in the anterior trunk, reaching a plateau of approximately constant length in the mid-trunk. In the posterior trunk, there is a striking decrease in somite length despite a constant somitogenesis period. In the tail, where period increases slightly, there is a further length decrease. This distribution of segment size may be adaptive for the specific hydrodynamic problems encountered by small larvae, allowing for a more flexible posterior body and thus a better anguiliform swimming mode (Webb and Weihs, 1986; Muller and van Leeuwen, 2004; McHenry and Lauder, 2006). However, because amniote mouse and chick embryos (Herrmann et al., 1951; Tam, 1981) show a strikingly similar profile of somite length along the axis, it seems likely that conserved developmental constraints also underlie this common feature of vertebrate somitogenesis.

In their natural habitats, developing zebrafish are exposed to a wide variety of temperatures (Engeszer et al., 2007). We show here that the distribution of zebrafish somite length along the axis is independent of the steady state developmental temperature. Changes in the period of somitogenesis due to temperature are coordinated with altered growth such that the proportions of the segments are maintained: in other words, segment length throughout somitogenesis is temperature-compensated. In the *Drosophila* embryo, the spatial positioning of segment borders is also temperature-compensated (Houchmandzadeh et al., 2002), and we expect that mechanisms that shield the proportions of poikilothermic embryos from the influence of developmental temperature will be essential.

The Clock and Wavefront Model in the Developing Embryo

The Clock and Wavefront model has been widely and successfully used to

Developmental Dynamics

interpret specific genetic and embryological perturbations of somitogenesis. In textbook illustrations of wild-type somitogenesis, oscillator period, somite length, and wavefront velocity are assumed to be constant along the axis—that is, the model's dynamics are at steady state (e.g., Wolpert, 2006). Cooke and Zeeman (1976) originally discussed the possibility that period, length, and wavefront might change during development. Here, we quantify the changes in these primary variables throughout somitogenesis of wild-type zebrafish. Thus, we provide a description of the process that can be used to adjust the steady state Clock and Wavefront model to the developing embryo.

The changes in somitogenesis period and somite length along the axis of the developing zebrafish are most striking in the tail, where segment length decreases as somitogenesis period increases. In a strict interpretation of the Clock and Wavefront model, an increase in somitogenesis period should result in longer rather than shorter somites. Our apparently paradoxical findings are resolved by postulating that the wavefront velocity also changes along the embryonic axis, independently from the somitogenesis oscillator period, and that its velocity slows strikingly in the posterior half of the embryo. Only in the central trunk are somitogenesis period and somite length, and hence wavefront velocity, all approximately constant. Therefore, in this region, the steady-state Clock and Wavefront model best approximates the situation in the developing embryo.

What are the cellular and molecular underpinnings of the observed changes in somitogenesis period and wavefront velocity along the axis? Both the clock and wavefront phenomena arise in the PSM. Convergence and extension movements and cell proliferation supply the PSM with cells, whereas the wavefront activity concomitantly diminishes the cell number in the PSM by arresting oscillations and gating cells anteriorly for differentiation. In embryos where tissue size has been artificially decreased, segment length adapts to the total length of tissue available, preserving the relative proportions of the embryo (Cooke, 1975; Tam, 1981). The initial purpose of the Clock and Wavefront model was to account for the apparent conservation of segment number under these circumstances by coupling the wavefront velocity to initial tissue size (Cooke and Zeeman, 1976). It is evident from our movies that the PSM size decreases significantly during somitogenesis (Fig. 4 and Supplementary Movie S3). We speculate that a mechanism continuously coupling the wavefront velocity to tissue size might be responsible for the decreasing somite length in a single embryo along the developing axis.

Gradients in signaling molecules produced in the tail bud have been invoked to position the wavefront during somitogenesis (Dubrulle et al., 2001; Sawada et al., 2001; Aulehla et al., 2003; Diez del Corral et al., 2003; Dubrulle and Pourquie, 2004b). The movement of the wavefront relative to the most recently formed somite is a function of the continuous posterior movement of the tail bud and the profile of the signaling gradients it generates. We expect that, in a PSM of decreasing size, the flux of signaling molecules from the posterior will diminish, resulting in altered profiles of signaling gradients. Thus, tissue size-dependent alterations in signaling flux might be one mechanism for coupling tissue size to wavefront movement. Similarly, period may be controlled by a factor that is synthesized in the tail bud in proportion to the resident cell number. Limited supply of the period-controlling factor in a continuously shrinking PSM might underlie the gradual increase in somitogenesis period in the tail.

In summary, our findings lead us to propose a modification of the steady-state Clock and Wavefront model in the zebrafish. The adjusted model does not alter its basic structure, but the specific values of its variables change in an axial- and temperature-dependent manner. The incorporation of the molecular and cellular dynamics of the PSM into the Clock and Wavefront model to explain these axial and temperature changes is the current challenge.

EXPERIMENTAL PROCEDURES

Preparation of Embryos, Molds

Zebrafish embryos were obtained by natural spawning. Wild-type embryos were AB strain if not otherwise stated. Tail somitogenesis was recorded from *nic*^{b107} homozygous embryos (Westerfield et al., 1990). Dechorionation was performed between shield and bud stage if necessary. Embryos were placed in depressions molded by silicone cones in 2% agarose/E3 in a Petri dish. Silicone cones were made as Sylgard 184 (Dow Corning) casts of custom-milled molds either produced from aluminum or Lucite. Two and two-tenths-mm-wide × 2.5-mm-deep conical wells were used for embryos with chorions or for dorsal viewing during early somitogenesis. Conical depressions 0.4 to 0.5 mm deep were used to analyze tail outgrowth. To observe anterior trunk somite formation, dechorionated embryos were oriented with the equator pointing toward the objective shortly before the start of recording. When measuring somitogenesis period in the anterior trunk, care must be taken to avoid temperature differences between incubator, dissection microscope, and time-lapse microscope. Embryos analyzed for tail outgrowth were oriented laterally around bud stage.

Generation of Time-Lapse Movies

Time-lapse series were recorded on a Zeiss Axioskop 200M with a ×5 Plan NEOFLUAR objective using standard brightfield optics. For tail outgrowth imaging, a ×0.63 tube lens (Zeiss TV2/3"C) was inserted in front of the camera. Images were acquired with a Photometrics Coolsnap HQ Camera. The microscope was equipped with a motorized stage (Zeiss MCU 28) driven by MetaMorph software (version 6.2r4, Universal Imaging Corp.). MetaMorph's MultiDimensional Acquisition tool was used to scan through up to 41 positions per experiment. For each position, a Z-stack consisting of five planes with 50 μm spacing was recorded. The time interval was one frame every 5 min, except for experiments at temperatures be-

low 25°C, where the sampling rate was reduced to 8 min.

ImageJ was used to produce focused and time-stamped movies. The ImageJ Stack Focuser plugin (http://rsb.info.nih.gov/ij/plugins/stack-focuser.html) selects and combines the in-focus areas from different Z-planes of one time point. All focused images from one position were combined into a time-stack, time-stamped, and saved both as a TIFF-stack and QuickTime movie. We wrote a multithreaded Java plugin, combining Stack Focuser, Time Stamper, and Movie Writer plugins to simultaneously process data from multiple embryos in parallel. This plugin is available from the authors upon request.

Determination of Somitogenesis Period and Somite Length

Somitogenesis movies were analyzed visually by annotating the time of somite boundary formation. A boundary was considered formed when it was clearly visible and spanned the tissue either from axial to lateral (dorsal view) or from dorsal to ventral (lateral view). If embryo angle precluded observing the somitic furrow as a dark line in lateral view, the appearance of a notch-like structure in the dorsal limit of the somitic mesoderm was considered indicative of boundary formation. To normalize for slightly different spawning times, we set the time at which somite boundary 6 formed to zero and calculated the times at which previous and following boundaries formed relative to this reference point.

For period measurements, 8 to 16 embryos were analyzed per experiment and view, and normalized mean formation time and SD for every boundary was calculated. We assigned the highest SD that was obtained in the experiment as the SD for formation time of somite 6. Somitogenesis period was determined by weighted linear regression using Origin software (OriginLab). Period values are given as the slope of the linear regression, errors represent the 95% confidence interval.

Somite length was measured in lateral view from focused TIFF-stacks in ImageJ. The program was calibrated using a 1 mm stage micrometer photographed with the same microscope settings. The length of each somite along the axis was measured from the frame in which it was first considered formed. A straight line was drawn connecting the intersections of the dorsal limit of the notochord with the two most recently formed somite boundaries. If embryo angle precluded observing the somitic furrow as a dark line, auxiliary lines connecting ipsilateral notch-like structures radially with the surface of the yolk ball were used as indicators of boundary position. The flattened geometry of the paraxial mesoderm in lateral view at the time of anterior segment formation prevented analysis of some segments. Between 8 and 12 embryos were measured in each length experiment. Somite lengths are stated as mean ± SD.

Temperature Experiments

The room with the time-lapse equipment was heated with an electric radiator (AKO-ISMET, type R909 TSIII); temperature regulation was achieved using a built-in air-conditioning system (Silent, Axair). Temperature inside the dish was measured with a K-type thermocouple dipped into the agarose and connected to a data logger system (Voltcraft Plus K202). It was re-calibrated using ice water and boiling water as references. Temperature values were recorded every minute. Mean temperature ± SD during the experiments is stated.

ACKNOWLEDGMENTS

We thank the Oates Lab, Saúl Ares, Luis Morelli, Ingmar Riedel-Kruse, Carl-Philipp Heisenberg, and Laurel Rohde for helpful discussions on the manuscript, the MPI-CBG fish facility for healthy and fertile fish, and Britta Schroth-Diez and the Howard Lab for help with microscopy. We acknowledge the mechanical workshop at MPI-CBG, Dresden, and Justin Costa and the NIH Mechanical Instrumentation Design and Fabrication branch. Healthy, adult *nic*^{b107} fish were provided by ZIRC. This work was supported by the Intramural Research Program of the National Human Genome Research Institute, National Institutes of Health.

REFERENCES

Aulehla A, Pourquie O. 2006. On periodicity and directionality of somitogenesis. Anat Embryol (Berlin) 211(Suppl)1:3–8.

Aulehla A, Wehrle C, Brand-Saberi B, Kemler R, Gossler A, Kanzler B, Herrmann BG. 2003. Wnt3a plays a major role in the segmentation clock controlling somitogenesis. Dev Cell 4:395–406.

Brooks S, Johnson IA. 1994. Temperature and somitogenesis in embryos of the plaice. J Fish Biol 45:699–722.

Bunning E. 1963. The physiological clock. Berlin: Springer-Verlag.

Cooke J. 1975. Control of somite number during morphogenesis of a vertebrate, *Xenopus laevis*. Nature 254:196–199.

Cooke J, Zeeman EC. 1976. A clock and wavefront model for control of the number of repeated structures during animal morphogenesis. J Theor Biol 58:455–476.

Diez del Corral R, Olivera-Martinez I, Goriely A, Gale E, Maden M, Storey K. 2003. Opposing FGF and retinoid pathways control ventral neural pattern, neuronal differentiation, and segmentation during body axis extension. Neuron 40:65–79.

Dubrulle J, Pourquie O. 2004a. Coupling segmentation to axis formation. Development 131:5783–5793.

Dubrulle J, Pourquie O. 2004b. fgf8 mRNA decay establishes a gradient that couples axial elongation to patterning in the vertebrate embryo. Nature 427:419–422.

Dubrulle J, McGrew MJ, Pourquie O. 2001. FGF signaling controls somite boundary position and regulates segmentation clock control of spatiotemporal Hox gene activation. Cell 106:219–232.

Engeszer R, Patterson L, Rao A, Parichy D. 2007. Zebrafish in the wild: a review of natural history and new notes from the field. Zebrafish 4:21–40.

Guryev V, Koudijs MJ, Berezikov E, Johnson SL, Plasterk RH, van Eeden FJ, Cuppen E. 2006. Genetic variation in the zebrafish. Genome Res 16:491–497.

Hanneman E, Westerfield M. 1989. Early expression of acetylcholinesterase activity in functionally distinct neurons of the zebrafish. J Comp Neurol 284:350–361.

Henry CA, Hall LA, Burr Hille M, Solnica-Krezel L, Cooper MS. 2000. Somites in zebrafish doubly mutant for *knypek* and *trilobite* form without internal mesenchymal cells or compaction. Curr Biol 10: 1063–1066.

Herrmann H, Schneider MJB, Neukom BJ, Moore JA. 1951. Quantitative data on the growth process of the somites of the chick embryo: linear measurements, volume, protein nitrogen, nucleic acids. J Exp Zool 118:243–268.

Holley SA. 2006. Anterior-posterior differences in vertebrate segments: specification of trunk and tail somites in the zebrafish blastula. Genes Dev 20:1831–1837.

Houchmandzadeh B, Wieschaus E, Leibler S. 2002. Establishment of developmental precision and proportions in the early

Drosophila embryo. Nature 415:798–802.

Jiang YJ, Aerne BL, Smithers L, Haddon C, Ish-Horowicz D, Lewis J. 2000. Notch signalling and the synchronization of the somite segmentation clock. Nature 408: 475–479.

Johnston IA, Vieira VV, Abercromby M. 1995. Temperature and myogenesis in embryos of the Atlantic herring *Clupea harengus*. J Exp Biol 198:1389–1403.

Kimmel CB, Ballard WW, Kimmel SR, Ullmann B, Schilling TF. 1995. Stages of embryonic development of the zebrafish. Dev Dyn 203:253–310.

Kulesa PM, Fraser SE. 2002. Cell dynamics during somite boundary formation revealed by time-lapse analysis. Science 298: 991–995.

Masamizu Y, Ohtsuka T, Takashima Y, Nagahara H, Takenaka Y, Yoshikawa K, Okamura H, Kageyama R. 2006. Real-time imaging of the somite segmentation clock: revelation of unstable oscillators in the individual presomitic mesoderm cells. Proc Natl Acad Sci U S A 103:1313–1318.

McHenry MJ, Lauder GV. 2006. Ontogeny of form and function: locomotor morphology and drag in zebrafish (*Danio rerio*). J Morphol 2006:1099–1109.

Muller UK, van Leeuwen JL. 2004. Swimming of larval zebrafish: ontogeny of body waves and implications for locomotory development. J Exp Biol 207:853–868.

Pearson M, Elsdale T. 1979. Somitogenesis in amphibian embryos. I. Experimental evidence for an interaction between two temporal factors in the specification of somite pattern. J Embryol Exp Morphol 51:27–50.

Pittendrigh CS. 1954. On temperature independence in the clock system controlling emergence time in *Drosophila*. Proc Natl Acad Sci U S A 40:1018–1029.

Riedel-Kruse I, Muller C, Oates A. 2007. Synchrony dynamics during initiation, failure, and rescue of the segmentation clock. Science 317:1911–1915.

Sawada A, Shinya M, Jiang YJ, Kawakami A, Kuroiwa A, Takeda H. 2001. Fgf/MAPK signalling is a crucial positional cue in somite boundary formation. Development 128:4873–4880.

Schmidt K, Starck JM. 2004. Developmental variability during early embryonic development of zebra fish, *Danio rerio*. J Exp Zoolog B Mol Dev Evol 302:446–457.

Schubert M, Holland LZ, Stokes MD, Holland ND. 2001. Three amphioxus *Wnt* genes (*AmphiWnt3*, *AmphiWnt5*, and *AmphiWnt6*) associated with the tail bud: the evolution of somitogenesis in chordates. Dev Biol 240:262–273.

Tam PP. 1981. The control of somitogenesis in mouse embryos. J Embryol Exp Morphol 65(Suppl):103–128.

van der Meulen T, Schipper H, van Leeuwen JL, Kranenbarg S. 2005. Effects of decreased muscle activity on developing axial musculature in *nic*^{b107} mutant zebrafish (*Danio rerio*). J Exp Biol 208:3675–3687.

van Eeden FJ, Granato M, Schach U, Brand M, Furutani-Seiki M, Haffter P, Hammerschmidt M, Heisenberg CP, Jiang YJ, Kane DA, Kelsh RN, Mullins MC, Odenthal J, Warga RM, Allende ML, Weinberg ES, Nusslein-Volhard C. 1996. Mutations affecting somite formation and patterning in the zebrafish, *Danio rerio*. Development 123:153–164.

Webb PW, Weihs D. 1986. Functional locomotor morphology of early life history stages of fishes. Trans Am Fish Soc 115: 115–127.

Westerfield M, Liu DW, Kimmel CB, Walker C. 1990. Pathfinding and synapse formation in a zebrafish mutant lacking functional acetylcholine receptors. Neuron 4:867–874.

Wolpert L. 2006. Principles of development. Oxford: Oxford University Press.

Wood A, Thorogood P. 1994. Patterns of cell behaviour underlying somitogenesis and notochord formation in intact vertebrate embryos. Dev Dyn 201:151–167.

Developmental Dynamics